Supporting Information

Impact of Repeated Temperature Cycling on the Low-Concentration CO_2 Adsorption Capacity of Grafted Silica-Amine

Charlotte M. Wentz, W. Sean McGivern, Maxwell D. Mevorah, Zois Tsinas, Jeffrey A. Manion, Amanda L. Forster*

Material Measurement Laboratory, National Institute of Standards and Technology, Gaithersburg, MD

*Email: amanda.forster@nist.gov

Table S1: Mass changes for fresh sample (triplicate and average value) converted to mmol N/g obtained from TGA temperature ramp analysis, based on the parent siloxylamine.

	Average	Measurements		
Sample		1	2	3
DAS/SBA-15	1.14 ± 0.05	1.21	1.10	1.11
TAS/SBA-15	0.960 ± 0.016	0.935	0.973	0.946
DAS/MCM-41	0.699 ± 0.014	0.727	0.692	0.707
TAS/MCM-41	1.43 ± 0.03	1.44	1.45	1.39

Table S2: CO_2 capacities at 5 % concentration in mmol g^{-1} (triplicate and average value) as measured with TGA.

	Average	Measurements		
Sample		1	2	3
DAS/SBA-15	0.869 ± 0.037	0.915	0.825	0.869
TAS/SBA-15	0.858 ± 0.014	0.829	0.856	0.859
DAS/MCM-41	0.631 ± 0.013	0.605	0.636	0.626
TAS/MCM-41	0.720 ± 0.034	0.792	0.714	0.726

Table S3: CO_2 capacities at 1 % concentration in mmol g^{-1} before and after an extended hold of the samples at 80 °C under a 50 cm^3 min^{-1} flow of dry CO_2-free air from a purge gas generator as measured with a TGA.

Sample	mmol/g Before	mmol/g After
DAS/SBA-15	0.57	0.57
TAS/SBA-15	0.57	0.60
DAS/MCM-41	0.50	0.49
TAS/MCM-41	0.64	0.66

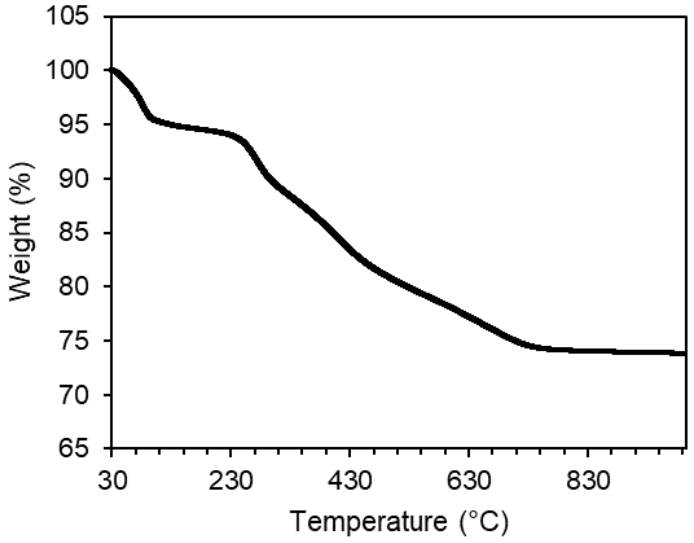

Figure S1: SBA-15 DAS 0 Cycles

.

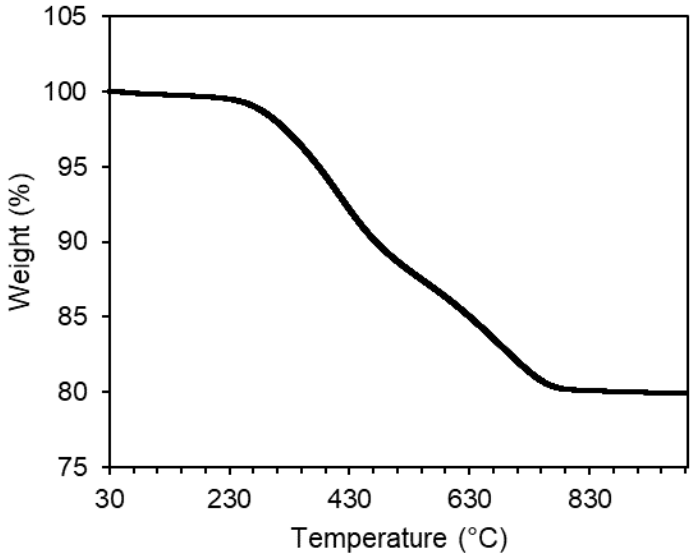

Figure S2: SBA-15 DAS 200 Cycles

.

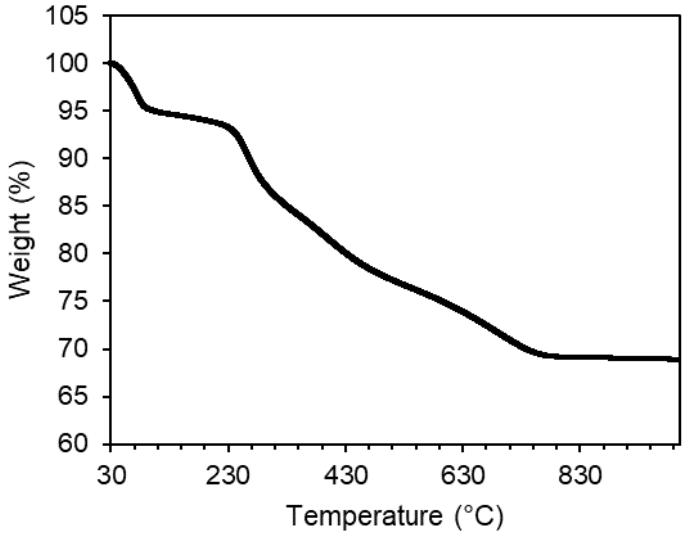

Figure S3: SBA-15 TAS 0 Cycles

.

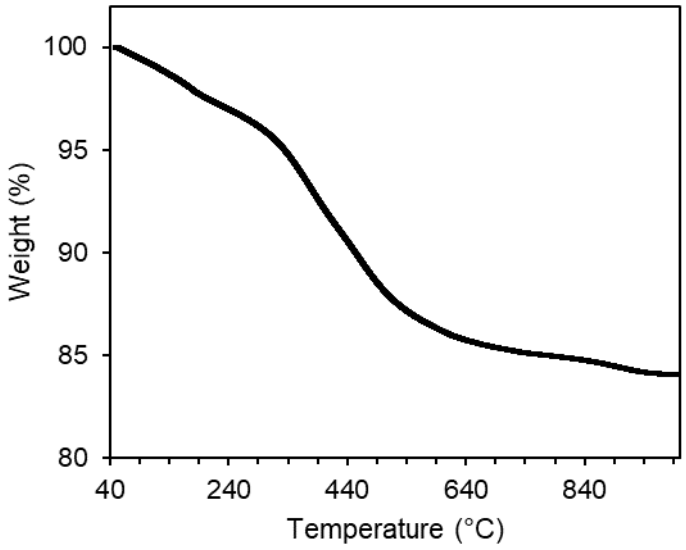

Figure S4: MCM-41 DAS 0 Cycles

.

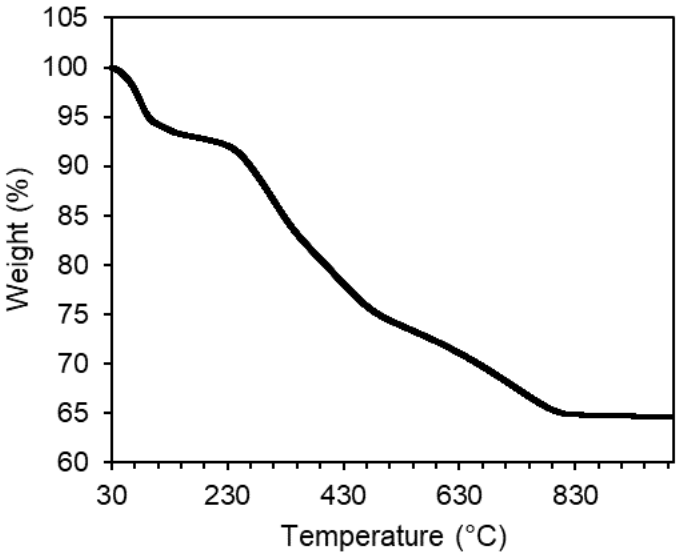

Figure S5: MCM-41 TAS 0 Cycles

.

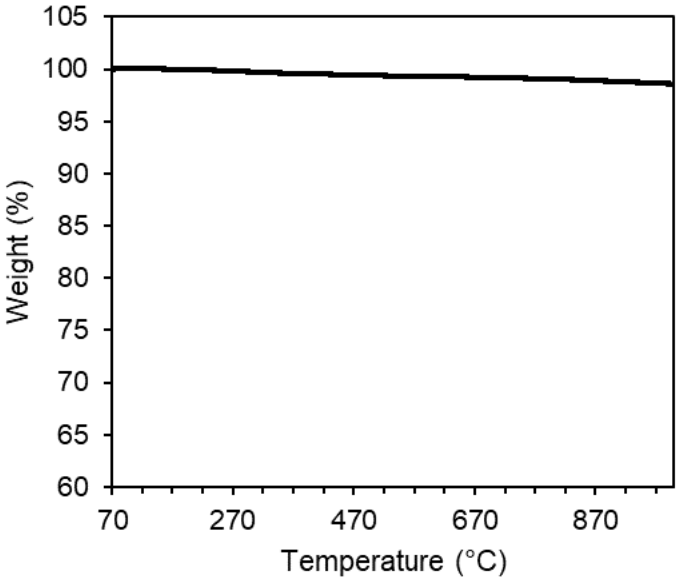

Figure S6: SBA-15 Neat

.

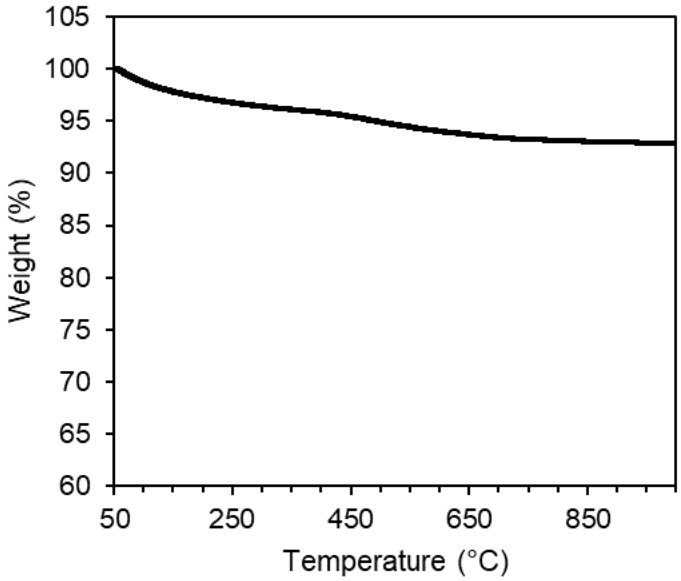

Figure S7: MCM-41 Neat

.

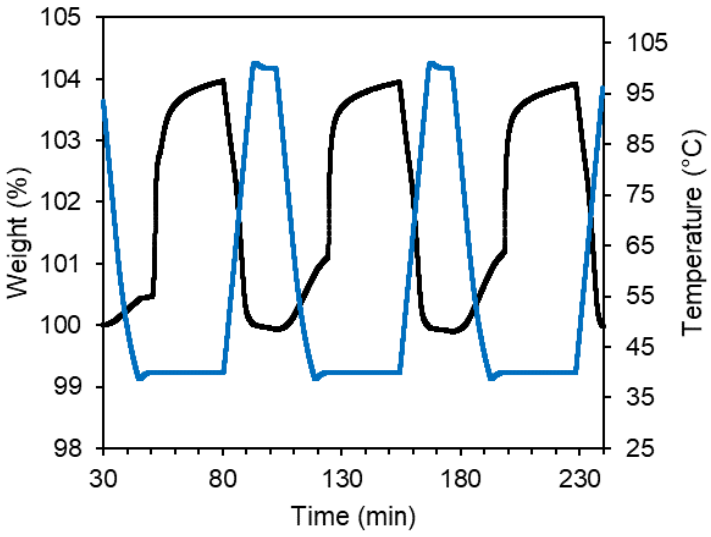

Figure S8: SBA-15 DAS Adsorption/Desorption in 5 % CO_2.

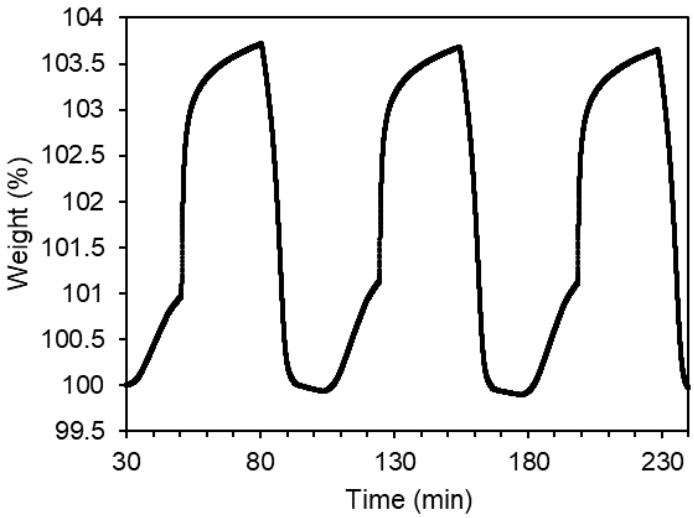

Figure S9: SBA-15 TAS Adsorption/Desorption in 5 % CO_2.

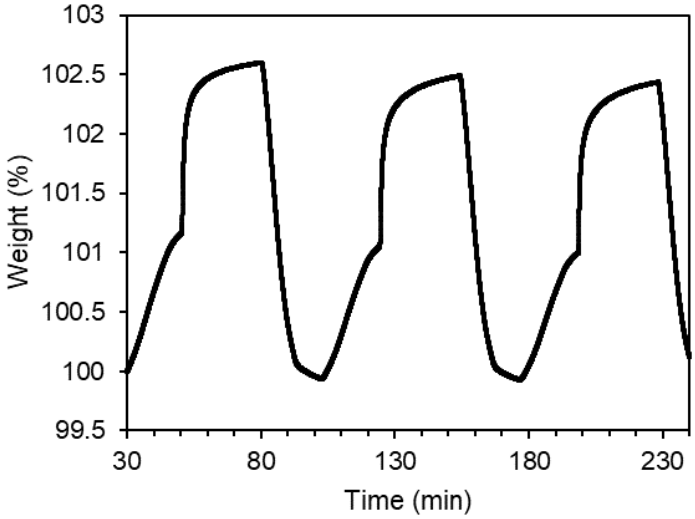

Figure S10: MCM-41 DAS Adsorption/Desorption in 5 % CO_2.

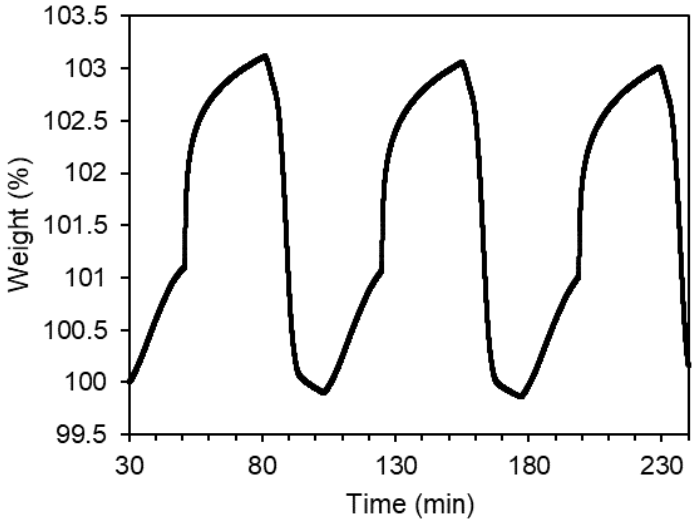

Figure S11: MCM-41 TAS Adsorption/Desorption in 5 % CO_2.

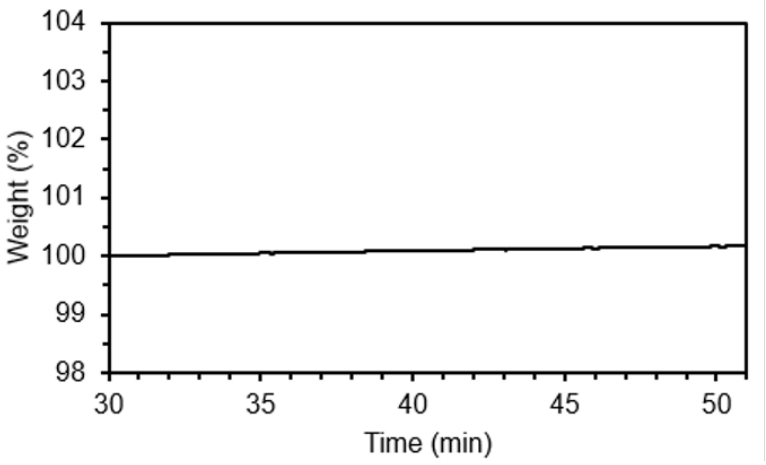

Figure S12: SBA-15 DAS Adsorption/Desorption in N_2; 0.180 % weight gain.

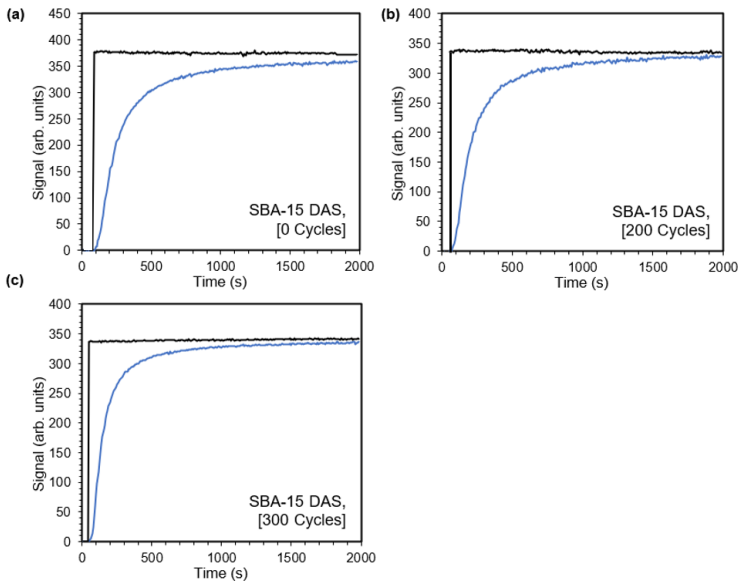

Figure S13: SBA-15 DAS dynamic column breakthrough at 400 µL L^{-1} CO_2.

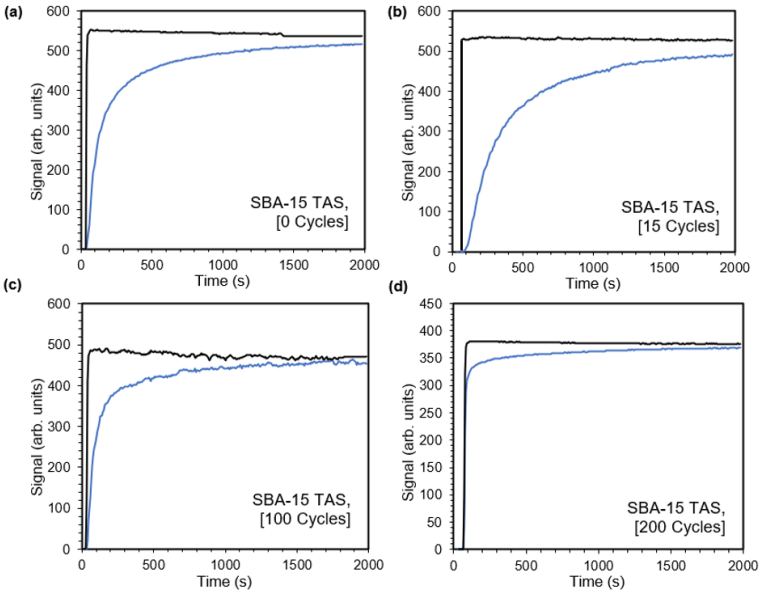

Figure S14: SBA-15 TAS dynamic column breakthrough at 400 µL L^{-1} CO_2.

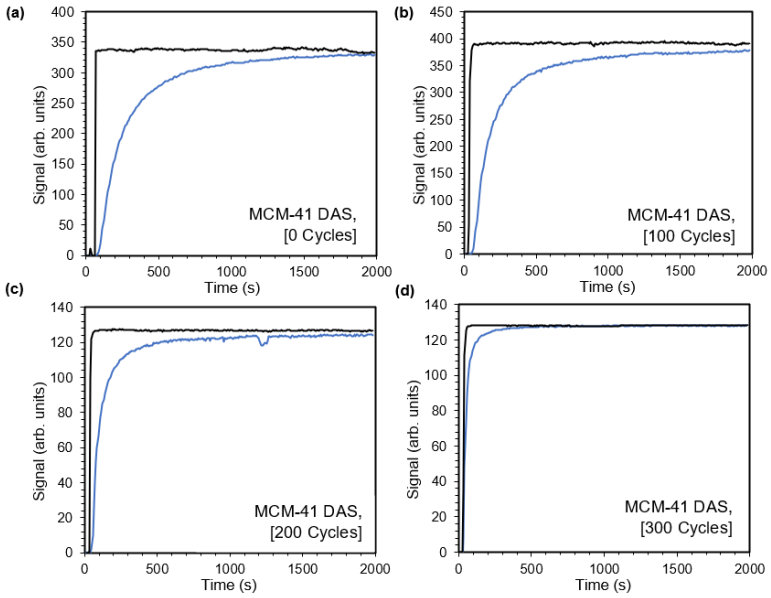

Figure S15: MCM-41 DAS dynamic column breakthrough at 400 µL L^{-1} CO_2.

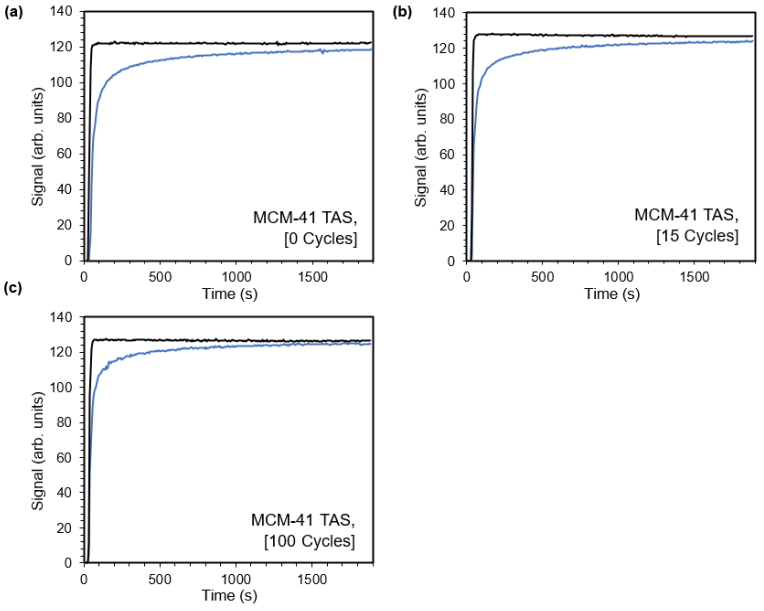

Figure S16: MCM-41 TAS dynamic column breakthrough at 400 µL L^{-1} CO_2.

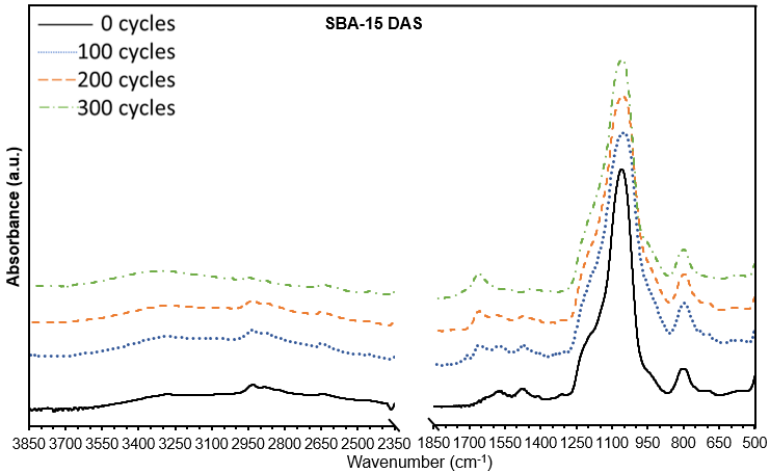

Figure S17: SBA-15 DAS FTIR.

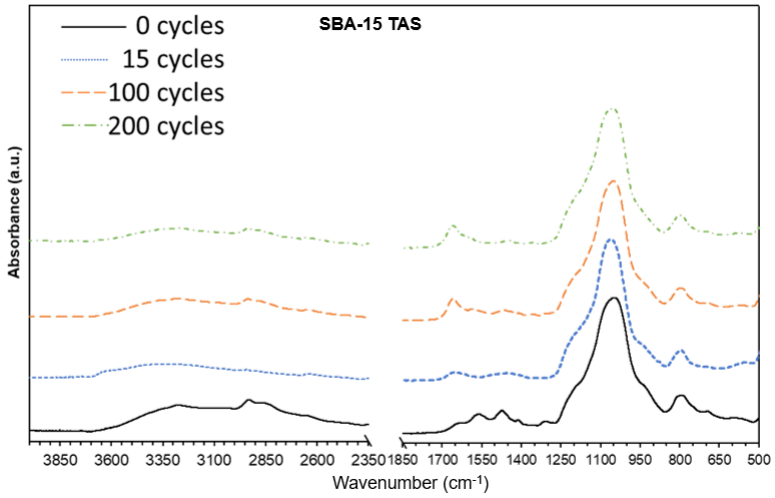

Figure S18: SBA-15 TAS FTIR.

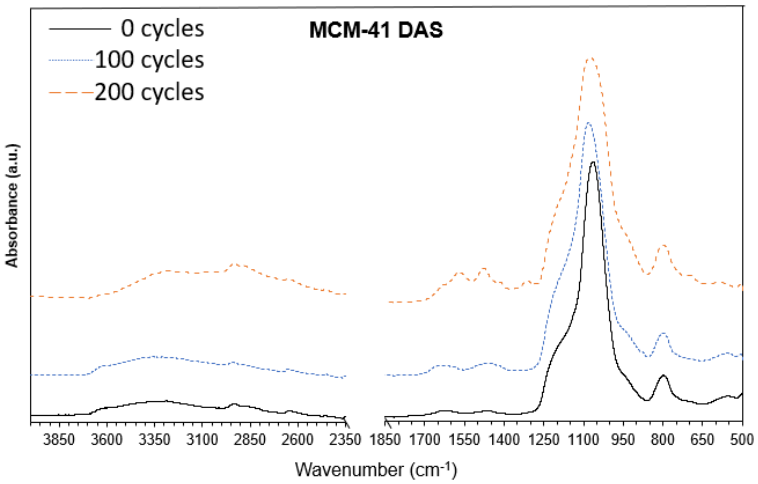

Figure S19: MCM-41 DAS FTIR.

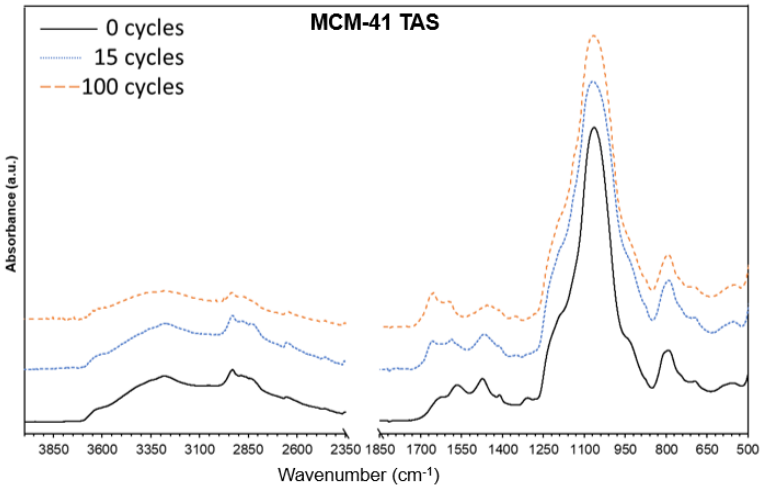

Figure S20: MCM-41 TAS FTIR.